THEORETICAL MODELLING OF ACCRETION DISK OSCILLATIONS*

Harshit Tiwari, Roll No. 191047
Supervisors: Prof. Pankaj Jain, Prof. J S Yadav
Department of Physics, IIT Kanpur - 208016, India
(Dated: April 18, 2021)

We study the normal modes of acoustic oscillations within thin accretion disks assumed to be non self-gravitating. Due to the relativistic effects, we use an effective Kerr potential to show that modes are trapped within and near the inner region of the disk. We study in depth the characteristics of epicyclic frequencies for rotating black hole. We find a correct dispersion relation for these modes and show that this relation is valid for $0 < a < 0.5$, up to a good approximation. We also discuss the regions where these acoustic modes might be trapped.

I. INTRODUCTION

Accretion being one of the most ubiquitous processes in astrophysics, describe the inflow of matter toward a central gravitating object. The structure of these accretion disks defines the properties of the central object. *In the case of a black hole, when the accreting gas gets close to it, the characteristics of radiation produced by it is strongly related to the spin of the hole and also to the presence of an event horizon.* Thus, analysing the luminosities and spectra of accreting black holes yields enticing evidence for both rotating holes and event horizons.

Normal modes of oscillations (similar to helioseismology modes existing within the sun) can be trapped within the region of strong gravity that exists in accretion disks near black holes. *They are a great tool to probe the nature of strong gravitational fields since these modes can't be found in Newtonian gravity.* We can determine both the mass and the dimensionless angular momentum parameter of the central black hole by analysing the spectrum of these modes.

In this paper, we use an effective Kerr potential to study the normal modes of acoustic oscillations and find out a dispersion relation. We also analyze the calculations done by Nowak and Wagoner (1991) [3] and see up to which interval of spin parameter a, our calculations make sense. The epicyclic frequencies for a test particle orbiting a rotating black hole, which are calculated using Kerr metric are discussed in depth, showing their radial distribution and characteristics near the inner region of accretion disk. We also discuss the regions where these oscillations can be trapped predicted by our dispersion relation,

II. METHODS AND TECHNIQUES DISCUSSION

With the work of Kato and Fukue (1980) [1], we know that oscillations can be trapped in the inner regions of accretion disks using suitable radial (κ) and vertical ($\Omega_\perp$) epicyclic frequencies whose explicit form can be found for free test particle orbiting the black hole. These epicyclic frequencies have been known for rotating black holes using suitable Kerr metric. The radial epicyclic frequency for prograde orbits is given by (Okazaki et al. (1987) [2]):

$$\kappa^2 = \frac{M}{r^3}\{1+\frac{a}{(\frac{r}{M})^{3/2}}\}^{-2}\{1-\frac{6}{\frac{r}{M}}+\frac{8a}{(\frac{r}{M})^{3/2}}-\frac{3a^2}{(\frac{r}{M})^2}\}. \quad (1)$$

Using Wolfram Mathematica, we graph this radial epicyclic frequency shown in Fig. 1. *From Fig. 1, we can see that $\kappa(r)$ reaches a maximum at small r and vanishes at the inner edge of the disk (shown for various values of a) which is not terminated by a stellar surface or magnetosphere, thus creating a resonant cavity where these modes are trapped.* The spectrum of this cavity thus reflects the properties of relativistic gravity as well as the physics of the inner accretion disk.

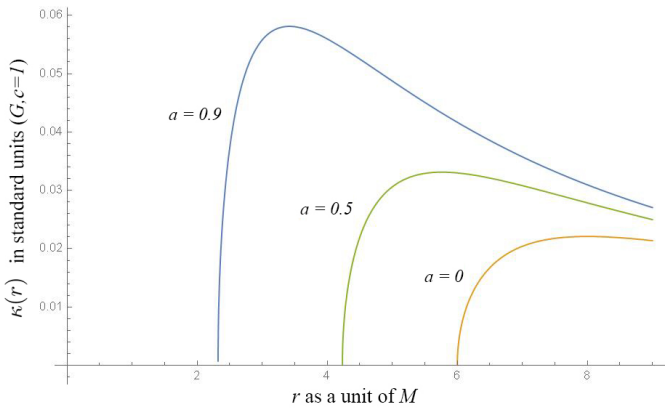

FIG. 1. Radial distribution of κ as a function of r for some a.

These modes are perturbations of the disk which has form $\boldsymbol{\xi}_* = \boldsymbol{\xi}(r,z)e^{i(\sigma t+m\phi)}$ (described as Lagrangian displacement) where r,z,ϕ are cylindrical coordinates, $\Omega(r)$

* Declaration: I hereby certify that the report has not been plagiarised or any part of it has not been copied from any other source or reference, and my supervisors approves this report.

is orbital angular velocity and a corotating frequency introduced as $\omega(r) = \sigma + m\Omega$, with σ eigenfrequency.

Nowak and Wagoner (1991) [3] analyzed the normal modes of acoustic oscillations within thin accretion disks where they used a modified Newtonian potential:

$$\Phi = -(M/r)[1 - 3(M/r) + 12(M/r)^2], \qquad (2)$$

which approximated the dominant relativistic effects near slowly rotating compact mass M.

II.1. The effective Kerr potential:

Here, we consider an *effective Kerr potential* (Fabian and Lasenby (2019) [4]) given by:

$$\Phi_{Kerr} = -\frac{M}{r} + \frac{1}{2r^2}[h^2 - a^2(k^2-1)] - \frac{M}{r^3}(h-ak)^2, \quad (3)$$

which we get by comparing the $\dot{r}^2$ equation (we got from solving the Kerr metric using Lagrangian method) with $1/2\dot{r}^2 + \Phi_{Kerr}(r) = const$. We see that (3) is equivalent to (2) for small a, while in general the second and third terms in (3) depend on h & k which are *specific angular momentum* and *energy* respectively. They have explicit form, for prograde orbits these are:

$$k = \frac{1 - \frac{2M}{r} + a\sqrt{\frac{M}{r^3}}}{\sqrt{1 - \frac{3M}{r} + 2a\sqrt{\frac{M}{r^3}}}}, h = \frac{\sqrt{Mr} - \frac{2aM}{r} + a^2\sqrt{\frac{M}{r^3}}}{\sqrt{1 - \frac{3M}{r} + 2a\sqrt{\frac{M}{r^3}}}}. \quad (4)$$

The innermost stable circular orbit is calculated when derivative of (3) vanishes and leads to $r^2 - 6Mr + 8a\sqrt{Mr} - 3a^2 > 0$. As we see, for $a = 0$, $r_{ISCO} = 6M$ while for $a = 0.998M$ i.e. for maximum attainable value, $r_{ISCO} = 1.24M$. We show the characteristics of Φ_{Kerr} for different values of a in Fig. 2., from which we can interpret that for large values of r ($r > 7M$), *the dependence of Φ_{Kerr} on a is negligible, and only for small values of r i.e. near the inner region of accretion disk, a dependence matters* (can also be seen by the fact that r_{ISCO} changes as a gets closer to its maximum attainable value).

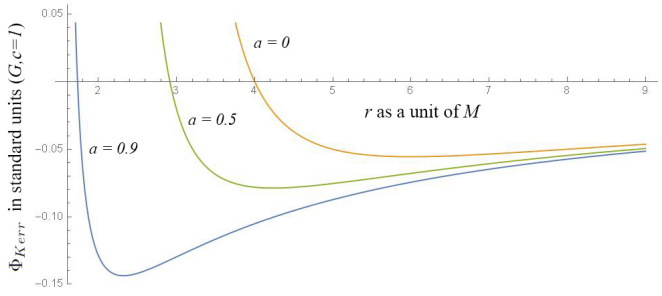

FIG. 2. Characteristics of Φ_{Kerr} for different values of a.

II.2. Adiabatic oscillations:

We consider a stationary axisymmetric unperturbed disk [3] to only have purely circular velocity, $v^\phi = r\Omega(r)$ ($\Omega(r)$ is angular velocity of disk rotation) and $v^r = 0$, thus $dM/dt = 0$ implies the negligence of viscous forces. Here, $\Omega(r)$ is a approximately a function of r only, since the condition that the gas is barotropic and inviscid, a combination of the r- and z- components of the equation of motion requires $\partial\Omega/\partial z = 0$. Note that r is now the cylindrical radial coordinate of our orthonormal basis which is different from the r dependence of (2) and (3) since both potential are spherically symmetric. The equations of equilibrium are:

$$r\Omega^2 = \partial\Phi/\partial r + \rho^{-1}\partial P/\partial r, \quad \rho^{-1}\partial P/\partial z = -\partial\Phi/\partial z, \quad (5)$$

while the adiabatic perturbations for this inviscid fluid flow with equation of state, $\Delta P/P = \gamma\Delta\rho/\rho$ satisfies:

$$(\partial_t + v^j\nabla_j)v^i + \rho^{-1}\nabla^i P + \nabla^i\Phi = 0, \qquad (6)$$

where v^i is fluid velocity, ρ and P are fluid density and pressure. Using the formalism developed by Lynden-Bell & Ostriker (1967) [3] we find a covariant description (eq.(2.7) in [3]) for a stationary non-self-gravitating Newtonian fluid, where the only post-Newtonian correction is in the potential. From this point, our calculations differ from that done by Nowak and Wagoner (1991) [3] who used the relativistic potential given in (2). We will use Φ_{Kerr} as Φ from now on to keep the notation simple unless specified.

The relativistic Keplerian frequency has explicit form (Kato (1990) [5]), $\Omega_K^2 = (M/r^3)(1 + aM^{3/2}/(8r^3)^{1/2})^{-1}$ whose distribution is shown in Fig. 3. As we can see, these frequencies are very close to each other for all values of r, whatever values a may take and can be approximated well by Keplerian angular velocity, $\Omega_K \approx \Omega_0 = M/r^3$.

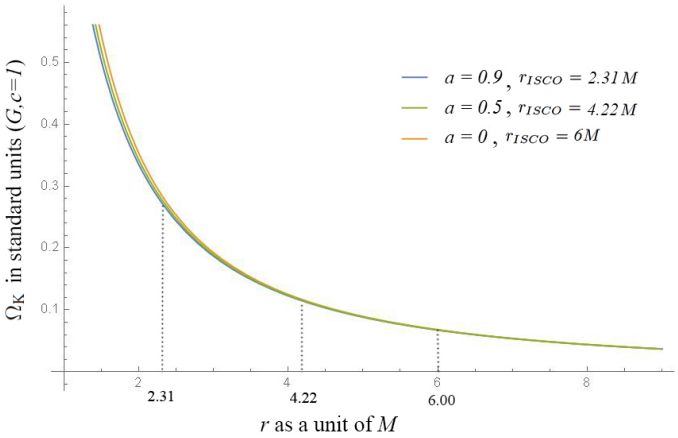

FIG. 3. Radial distribution of Ω_K as a function of r for some a. Here, the values of Ω_K actually terminates when $r < r_{ISCO}$, but to show the near relation of all 3 curves we haven't terminated them.

While, the frequency of vertical oscillations of fluid particles, $\Omega_\perp$, around the equatorial plane is (Kato (1990 [3])):

$$\Omega_\perp^2 = \Omega_K^2(1 - \frac{4a}{(r/M)^{3/2}} + \frac{3a^2}{(r/M)^2}). \tag{7}$$

This vertical epicyclic frequency does changes as a increases unlike the above mentioned Keplerian frequency as shown in Fig. 4. This and the fact that effective Kerr potential is also spherically symmetric, in cylindrical coordinates, near $z = 0$, taking the *radial cylindrical derivative*, we expect:

$$\frac{\partial\Phi}{\partial r} = r\Omega_\perp^2[1 + \frac{z^2}{2r^2}\frac{\partial \ln \Omega_\perp^2}{\partial \ln r} + \mathcal{O}(z/r)^4], \tag{8}$$

which was calculated for any general spherically symmetric potential with corresponding vertical frequency, where previously we used Ω_0 in place of $\Omega_\perp$ which are both equal for non-rotating central objects. Solving the above mentioned covariant equation (eq.(2.7) in [3]) in the cylindrical orthonormal basis, we obtain the famous *structural equations* (eq.(2.8) in [3]) for thin disks having no radial or vertical component of velocity. The only change we have made is using $\Omega_\perp$ in place of Ω_0.

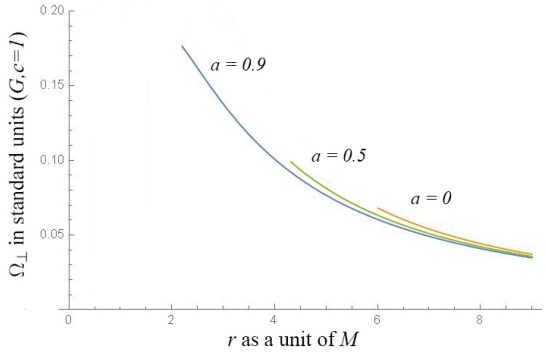

FIG. 4. Radial distribution of $\Omega_\perp$ as a function of r for some a.

We also analyse the relation between $\partial\Phi_{Kerr}/\partial r$ and $r\kappa^2$ in Fig. 5., which shows that for small values of a ($a < 0.5$), the radial partial derivative of Kerr potential is correctly approximated by the radial epicyclic frequency ($r\kappa^2$), which we expected. For larger a, we need to get a better approximation.

II.3. The dispersion relation:

We restrict ourselves to the perturbation of thin disks in hydrostatic equilibrium, where $\rho^{-1}\partial P/\partial z = -\partial\Phi/\partial z$ from (5) and $\partial\Phi/\partial z = \Omega_\perp^2 z$ calculated using (8). In the lowest WKB order in λ/r where λ is radial scale length given by, $\lambda = 2\pi|\xi^r/(\partial\xi^r/\partial r)|$, where for thin disk models, $h \lesssim \lambda \ll r$ and $\lambda\omega \sim c_s(\sim h\Omega)$. Here, h is effective half-thickness of unperturbed disk and c_s is speed of sound given by, $c_s = (\gamma P/\rho)^{1/2}$. To this order, $\Omega^2(r) = \Omega_\perp^2(r)$

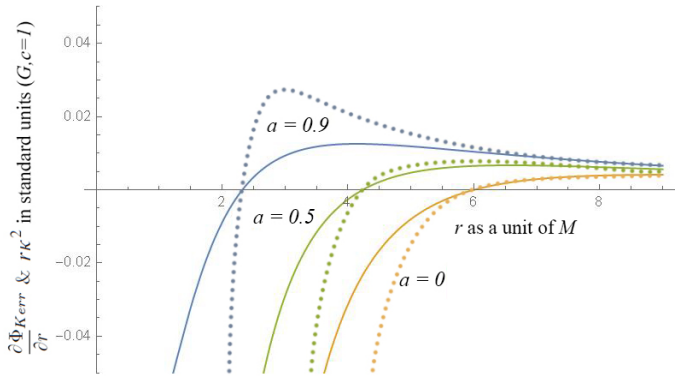

FIG. 5. Comparison of $\partial\Phi_{Kerr}/\partial r$ and $r\kappa^2$ where r is the spherical polar coordinate and not the cylindrical one. Dotted line shows $\partial\Phi_{Kerr}/\partial r$ while the other one is $r\kappa^2$ for corresponding values of a. Here, the values of of all curves actually terminates when $r < r_{ISCO}$.

and we get the "WKB versions" of structural equations (eq.(2.8) in [3]) given by eq.(3.1) in [3]. Here, the radial epicyclic frequency is different, given by:

$$\kappa^2 = 4\Omega_\perp^2 + r\frac{\partial\Omega_\perp^2}{\partial r} \tag{9}$$

On solving these "WKB versions" of structural equations by expanding the Lagrangian displacement about $z = 0$, we get the differential equation:

$$\nu_r\nu_{z(J-1)}\xi_j^r + \frac{h^2}{\gamma}\frac{\omega^2}{\Omega_\perp^2}\frac{\partial^2\xi_j^r}{\partial r\partial r_m} = 0, \tag{10}$$

where, $\partial/\partial r_m \equiv \partial/\partial r - 2m\Omega_\perp/\omega r$, $\nu_r \equiv (\omega^2 - \kappa^2)/\gamma\Omega_\perp^2$, and $\nu_{z(j)} \equiv (\omega^2 - (1+j)\Omega_\perp^2)/\gamma\Omega_\perp^2$. This leads to the new *dispersion relation* given by:

$$(\omega^2 - J\Omega_\perp^2)(\omega^2 - \kappa^2) = \omega^2 c_s^2 k^2, \tag{11}$$

where $\Omega_\perp$ and κ are given by (7) and (1) respectively. Since, the R.H.S in (11) is always positive, we have two cases of trapped oscillations: for regions where $\omega^2 < \kappa^2$ and $\omega^2 < J\Omega_\perp^2$ and for regions where $\omega^2 > \kappa^2$ and $\omega^2 > J\Omega_\perp^2$.

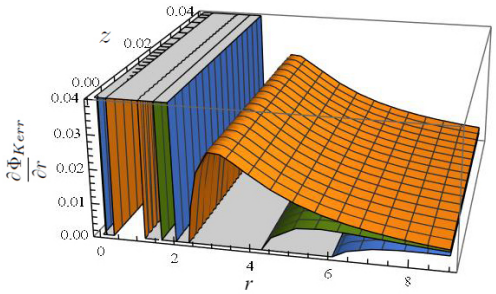

FIG. 6. Characteristic of $\partial\Phi_{Kerr}/\partial r$. Here, r and z are the cylindrical coordinates, measured in units of M. Orange, green and blue surfaces shows the graph for $a = 0.9$, $a = 0.5$ and $a = 0$ respectively.

This result (11) have been calculated after considering proper coordinate transformation between spherical and cylindrical coordinate and we show in Fig. 6., the characteristic of $\partial\Phi_{Kerr}/\partial r$ in cylindrical coordinate and see that near $z = 0$, the z-dependence of $\partial\Phi_{Kerr}/\partial r$ is negligible, while arguing from the point made earlier in Fig. 5., the result (11) holds true to a great approximation up to $a = 0.5$, while for larger values of a, for e.g. $a = 0.9$, we see the relation (8) will no longer be true.

III. RESULTS AND DISCUSSION

We find a dispersion relation in (11). For the regions, $\omega^2 > \kappa^2$ and $\omega^2 > J\Omega_\perp^2$, the normal modes of oscillations are mainly acoustic (due to pressure), where they extend a small distance from the inner regions of the disk. We see that for $r > r_{ISCO}$, (8) holds very true for low values of a, $0 < a < 0.5$, while for $r \gg r_{ISCO}$, i.e. for the large outer region of the disk, (8) holds even for larger values of a (interpreted from Fig. 5.). *Thus, acoustic (pressure) modes can be trapped near a small distance from inner region of the disk and even in the large outer region of the disk.*

For the regions, $\omega^2 < \kappa^2$ and $\omega^2 < J\Omega_\perp^2$, modes can be trapped near the region where κ becomes maximum, but these are not acoustic in nature as discussed by Nowak and Wagoner (1992) [6] but rather wholly due to gravity as we expect from studying the characteristics of epicyclic frequencies, since near r_{ISCO}, they all shows large variation.

We can use this result to analyse different binary systems, like GRS 1915+105 shown to have the low frequency QPO's varying just as the dynamic frequency (the inverse of the sound crossing time) by Misra et al. (2019) [7]. The spectrum of X-ray binary systems contains various modes of oscillations and some of these are acoustic in nature, trapped at various radii from the inner most stable circular orbit and this result can be used to study some of these trapped oscillations, as we discussed the region and interval of a in which (11) makes sense.

IV. SUMMARY AND CONCLUSIONS

Using an effective Kerr potential, we find a dispersion relation (11) which correctly describes the normal acoustic modes of oscillations for $\omega^2 > \kappa^2$, which hold true up to a good approximation for $0 < a < 0.5$.

[1] S. Kato and J. Fukue, Trapped Radial Oscillations of Gaseous Disks around a Black Hole, 1980PASJ...32..377K.

[2] Okazaki, A. T., Kato, S., Fukue, J, Global trapped oscillations of relativistic accretion disks, 1987PASJ...39..457O.

[3] Nowak, Michael A.; Wagoner, Robert V., Diskoseismology: Probing Accretion Disks. I. Trapped Adiabatic Oscillations, 1991ApJ...378..656N.

[4] Andrew C. Fabian, Anthony N. Lasenby, Astrophysical Black Holes, arXiv:1911.04305.

[5] Kato, S., Trapped one-armed corrugation waves and QPOs, 1990PASJ...42...99K.

[6] Nowak, Michael A.; Wagoner, Robert V., Diskoseismology: Probing Accretion Disks. II. G-Modes, Gravitational Radiation Reaction, and Viscosity 1992ApJ...393..697N.

[7] Ranjeev Misra, Divya Rawat, J S Yadav, Pankaj Jain, Identification of QPO frequency of GRS 1915+105 as the relativistic dynamic frequency of a truncated accretion disk arXiv:2001.07452.